كلية الهندسة بشبرا
FACULTY OF ENGINEERING AT SHOUBRA
ERJ
PRINT ISSN 3009-6049
ONLINE ISSN 3009-6022

ENGINEERING RESEARCH JOURNAL (ERJ)
Volume (53) Issue (3)
Jul. 2024, pp:73-90
https://erjsh.journals.ekb.eg

Optimizing Ultra High-Performance Concrete Mixtures Adopting the Modified Andreassen Approach

M. Abdelkarim[1*], Mohamed S. Saif[1], Gehan Hamdy[1], Hossam Z. El-Karmoty[2], M. O. Ramadan[1], Mohamed R. Sakr[1]

[1] Department of Civil Engineering, Faculty of Engineering at Shoubra, Benha University, Cairo, Egypt
[2]Housing & Building National Research Institute (HBRC).
[*] Corresponding Author.
E-mail: **Mahmoud.abdelkareem@feng.bu.edu.eg, mohamed.ismaeel@feng.bu.edu.eg, Osama.alhariri@feng.bu.edu.eg, Gehan.hamdy@feng.bu.edu.eg, Hoskarmoty@yahoo.com, ahmed.khater@feng.bu.edu.eg**

Abstract: This paper addresses the mixture design and assessment of properties related to cost-effective ultra high-performance concrete (UHPC), targeting densely compacted cementitious matrices. The modified Andreasen and Andersen particle packing model was employed to define boundaries between binder and aggregate content. Optimization was initially performed for mortar followed by concrete. Mortar mixtures involved ternary replacement of cement by silica fume, metakaolin and limestone at various volume percentages of 35% to 55%. Adding basalt to mortar allowed 20-30% volume replacement to obtain a unique UHPC mixture that satisfied the requirements of particle packing models and performance-based approaches with minimal impact of compressive strength. The results show that the modified Andreasen and Andersen particle packing could represent the formwork of UHPC mixture design while the performance-based approach is necessary to reach the optimum mix. The addition of 2% volumetric ratio of short double-headed steel fibers improved the compressive and tensile strengths by up to 13% and 50%, respectively. Steam curing accelerated the gain of concrete strength compared to normal and hot curing methods.

Keywords: Ultra High-Performance Concrete; Modified Andreassen Model; Mixture Optimization; Particle Packing; Steel Fibers.

1. Introduction

Ultra-high-performance concrete (UHPC) is a recently developed type of concrete that has a great potential for intensive future implementation in the construction industry due to the remarkable properties and advantages it imparts over conventional concrete [1]. UHPC is highly workable with unique compressive strength features (100-150 MPa) and robust ability to resist aggressive environments (e.g. sulfate attack and chloride ingress), making it an advisable selection for special applications e.g. bridges, dams, tunnels, pavements, offshore structures, and repair [2-4].The fundamental concept behind UHPC was to produce concrete with highly compacted microstructure and minimal voids through a significant reduction of gel pores (less than 10 nm), capillary pores (100-1000 nm), and interfacial zones [5-6]. Enhanced packing density in UHPC caused increased contact area among particles which stimulated lower stress transfer, decreasing the formation of microcracks and improving mechanical characteristics.

Constituent materials of UHPC vary according to the designated performance and application but typically combine cement, supplementary cementitious materials (SCMs) and filling aggregates, with significantly low water-to-binder ratio (*w/b*) less than 0.25 and the addition of high-range water-reducing superplasticizers to maintain desirable fluidity and workability levels [7]. Although similar in components to normal concrete, UHPC typically contains larger proportions of cement (800-1200 kg/m^3) imposing serious environmental risk due to higher carbon footprint related to cement production and excessive expenditures [8], thus obstructing its wide application. Accordingly, research targeted reducing cement content in such concrete through two main techniques; incorporating viable alternatives obtained from industry wastes (i.e. SCMs) and re-shaping aggregate grading by adopting particle packing density models. SCMs could refine pore sizes and improve packing density through the filling effect and/or deposition of binding materials into the pore system [9]. For instance, the addition of silica fume to UHPC formed calcium silicate

hydrate (C-S-H) gel, providing seeding locations for cement hydration products, and a higher packing effect imparted by un-dissolved silica particles [10]. Metakaolin contributed to UHPC in a similar pattern as silica fume but typically forms C-S-H and calcium aluminate hydrate (C-A-H) phases and may result in higher consumption of CH [11]. Fly ash (FA) was also employed in UHPC affecting positively the workability of mixtures, but its coarser particles provided an insignificant seeding effect compared to silica fume or metakaolin, thus producing comparatively lower strength. Limestone powder (LP) was also suggested as a substitute for micro fillers in UHPC to improve workability due to its fine spherical particles and enhance strength properties by filling and nucleation effects [11-13].

Combining coarse aggregates in UHPC mixtures reduces the needed binder content and eliminates the shrinkage drawbacks. The majority of UHPCs were created with refined aggregate grading to overcome the inherent weaknesses of the coarse aggregate and paste matrix, decrease stress concentration at areas of contact between aggregates and avoid the intrinsic strength limit of coarse aggregate [7]. According to Ma *et al.* [14], coarse aggregate can reduce material costs, improve workability, and increase the elastic modulus of UHPC. Li *et al.* [15] reported that the ideal powder content is determined to be around 800 kg/m^3 and 700 kg/m^3 for basalt with a maximum size of 8 mm and 16 mm, respectively. His remarks were in good agreement with predictions by the modified Andreassen approach to optimize the particle distribution and achieve the highest possible density from mixed constituents.

Despite the wide range of constituent materials that can be incorporated into UHPC to assist with the development of more sustainable UHPC and less polluted ecosystems, a challenge has been imposed to design UHPC mixtures incorporating basalt coarse aggregates, which requires optimization towards the required performance criteria. Particle packing theory approaches were used intensively to design optimized concrete mixtures since the theory aimed to minimize porosity by introducing smaller particles into interstitial spaces between larger ones and reducing voids. Particle size distribution, shape, and processing method are the main factors of different packing approaches. The Modified Andreassen particle packing model was trusted among researchers in the realm of UHPC [8,15-18].

Conversely, Meng *et al.* [19] relied on the performance-based design approach and reported that the theory of maximum packing density fails to identify the actual particle distribution due to the existence of inter-particle forces for very fine particles of cement and SCMs. Furthermore, the introduction of liquid into the mixture has an impact on the contact force between tiny particles measuring less than 100 µm [20]. The performance-based approach is a multi-step design in which various cement and SCMs ratios were considered to obtain the most promising cement paste, then aggregates and/or steel fibers were added at different percentages to form the UHPC mixture. However, this trial-and-error method is a physical approach with the introduction of aggregates into UHPC paste has the potential to disturb the particle packing and thereby significantly impacts its workability and compressive strength. The compaction of both aggregates and powder materials is a crucial factor in determining the performance of UHPC.

The current experimental investigation aimed to create a cost-effective UHPC mixture based on a design procedure that has the features of a performance-based design approach and its boundaries defined based on the particle packing theory of the modified Andreassen model.

1.1. Modified Andreassen model

According to the Modified Andreassen model,

$$CPET = \left(\frac{d^q - {d_o}^q}{D^q - {d_o}^q}\right) * 100 \qquad (1)$$

where,

CPET = the cumulative (volume) percent finer than sieve size, d = the particle size, d_o = the minimum particle size of the distribution, D = the maximum particle size, and q = the distribution coefficient or exponent usually from 0.19 to 0.23 for UHPC mixes. In this investigation q was taken as 0.22 [15,21]

2. Experimental Program

2.1. *Materials*

Ordinary Portland cement (OPC) with a grade of 52.5N, silica fume (SF), metakaolin (MK) and limestone powder (LP) were used as the main binders for mortar and concrete specimens. The physical and chemical properties of employed binders are provided in Table 1. Also, Figure 1 shows the particle size distribution for the used binders.

Table 1. Chemical Composition and Physical Properties of Binder Constituents.

	OPC	SF	MK	LP
Chemical composition				
SiO_2 (%)	21.2	96.0	55.0	3.6
Al_2O_3 (%)	5.5	0.1	42.1	0.3
Fe_2O_3 (%)	3.2	1.0	1.4	0.2
CaO (%)	63.4	0.2	0.3	53.3
MgO (%)	0.7	0.2	0.3	0.8
K_2O (%)	0.5	0.2	-	0.4
SO_3 (%)	2.4	0.1	-	0.1
$Na_2O_{eq.}$ (%)	0.1	0.1	0.9	0.0
Physical properties				
D10, µm	1.50	0.08	0.027	0.02
D50, µm	9.30	0.22	0.06	0.40
D90, µm	45.0	2.00	0.11	6.00
Specific gravity	3.15	2.15	2.5	2.65
Loss on ignition (L.O.I) (%)	3.0	2.1	0.9	4.1

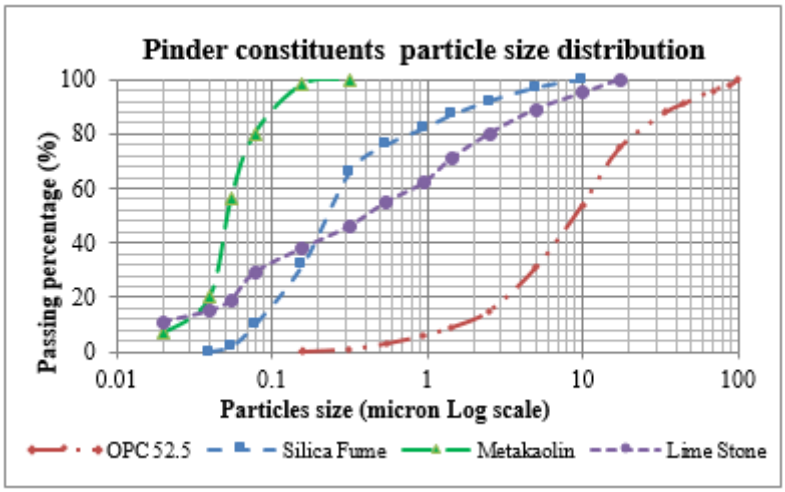

Fig 1. Particle Size Distribution of Used Binders.

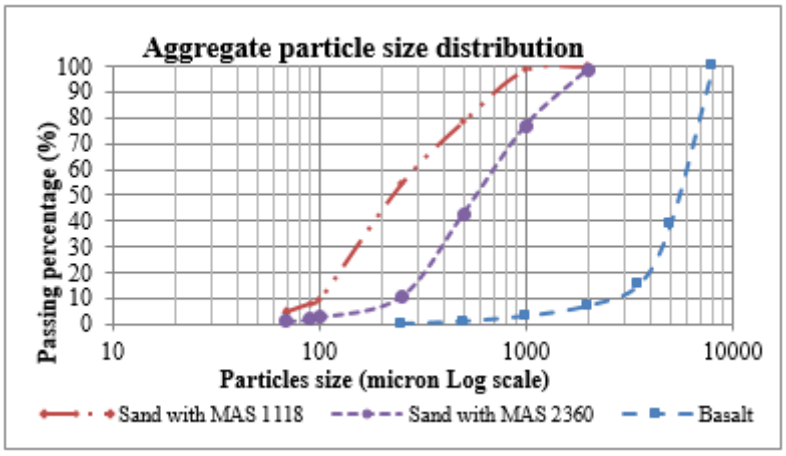

Fig 2. Particle Size Distribution of Used Sand and Basalt.

Two sets of fine aggregate (sand) were used which did not exhibit chemical reactivity during the process of cement hydration; one with a maximum size of 2.35 mm and another of 1.18 mm (as shown in Figure 2) with a fineness

modulus of 2.66 and 1.7 respectively, absorption of 1.0% and specific gravity of 2.65. For concrete specimens, basalt was employed as coarse aggregate with a maximum size of 10mm (as shown in Figure 2) which had a specific gravity and absorption of 3.0 and <1.0%, respectively. In addition, one concrete mixture comprised hooked macro steel fibers (at a dosage of 2% of concrete volume) with a length and diameter of 30 mm and 0.4 mm, respectively, and a corresponding aspect ratio of 75. The specific gravity, elastic modulus, and tensile strength of steel fibers were 7.85, 205 GPa, and 1350 MPa, respectively. A target workability of 190mm [22] was achieved using a polycarboxylate-based high-range superplasticizer (Master Glenium SKY3888) at the recommended dosage of 0.5-3.0 liter/100kg of binder content.

2.2. Mixture Design

As recommended in the literature, mixtures were designed according to the performance-based design approach employing the framework of modified Andreassen particle packing theory [20,23] Eight total mixtures were cast in two distinct phases. Initially (Phase I), four mortar mixtures were designed to provide a guideline for Phase II which involves four ultrahigh-performance concrete mixtures. In this study, the Modified Andreassen model used a distribution coefficient (q) of 0.22 [15].

2.2.1. Phase I: High-performance mortar design

Saif *et al.* [24] manufactured self-compacting high-strength concrete by employing a quaternary binder approach (cement, silica fume, metakaolin and limestone). Optimum fresh and mechanical qualities were obtained at 15% silica fume, 5% metakaolin and 20% limestone (40% replacement ratio). The prescribed mixture represented the basis of the current study as shown in Table 2.

This mixture was subjected to a design process to obtain the most favorable ratios of binder and sand with the modified Andreassen curve as a basis. Four different mixtures were suggested as shown in Tables 3 and 4, following these methodology/criteria:

1- Ideal modified Andreassen curves as shown in Figure 3 were developed by restricting the maximum size of sand to 1.18 mm (1180 microns) and 2.35 mm (2350 microns). The distribution coefficient (q) was fixed at 0.22 [15].
2- To improve the efficiency of using cement, a ternary blend of silica fume, metakaolin and limestone with weight ratios of around 3:2:1 was used [24] [25].
3- The upper limit for the particle size of the binder, composed of cement, silica fume, metakaolin and limestone was 90 microns; accordingly, the passing percentage of 90 μm sieve represented the total binder percentage. Results shown in Figure 3 led to deciding the amount of binder in mortar particles as 40% and 50% for maximum sand size of 2350 and 1180 microns, respectively.
4- Cement replacement percentage was carefully chosen to ensure a cement content within the range of 550-680 kg/m^3. Thus, cement replacement ratios under consideration were 35% 45% and 55% based on binder volume.
5- The water-to-binder ratio (w/b) was maintained at a consistent value of 0.20 while target workability (minimum slump of 190mm) was achieved by the addition of a superplasticizer with a volume percentage ranging from 1.7% to 2.0%
6- Following the selection of the appropriate volume percentage for the binders and aggregate, paste volume was estimated relative to the aggregate volume.

Table 2. Components of Reference Mixture (kg/m^3).

C	LS	SF	MK	B	CA	FA	W	S.P	W/C	W/B	S.P/C	S.P/B	(LS+SF+M)/B
660	220	165	55	1100	540	590	200	43	30%	18%	1.6%	1.4%	40%

C= Cement, LS= Limestone, SF=Silica Fume, MK= Metakaolin, B= Total binder, CA= Basalt, FA= Sand with max. size 0.6mm, W= Water, S.P= Superplasticizer

Table 3. Components Of Mortar Mixtures by Weight (kg/m^3)

Mix#	Code	C	LS	SF	MK	FA	W	S.P	B	B:FA	W/B
M1	50M35	665	140	92.2	45.5	1282*	180	18.85	942.7	42% : 58%	0.20
M2	50M45	563	186	124	62	1282*	176	18.7	935	42%: 58%	0.20
M3	60M45	675	223	150	74.1	1023**	211	22.5	1122.1	52% : 48%	0.20
M4	60M55	552	258	168	87.7	1037**	205	21.3	1065.7	51% : 49%	0.20

C=Cement, Ls=Limestone, S=Silica Fume, M=Metakaolin, FA*=Sand with max. size 2.35mm, FA**=Sand with max. size 1.18mm, W=Water, S.P=Superplasticizer, and B= Total binder content

Table 4. Components Of Mortar Mixtures by Volume (%)

Mix#	Code	C	LS	SF	MK	FA	W	S.P	B	B:FA	W/B	PV
M1	50M35	21.0	4.3	5.2	1.8	48.0	18.0	1.7	32.3	40: 60	58	52
M2	50M45	17.7	6.9	5.7	2.5	47.9	17.6	1.7	32.8	41: 59	56	52
M3	60M45	21.0	8.3	6.8	2.9	37.9	21.1	2.0	39.0	51 : 49	57	62
M4	60M55	17.5	9.7	7.8	3.5	39.1	20.5	1.9	38.5	50: 50	56	61

C=Cement, Ls=Limestone, S=Silica Fume, M=Metakaolin, FA=Sand, W=Water, SP=Superplasticizer, B= Total binder content , and PV= Paste volume.

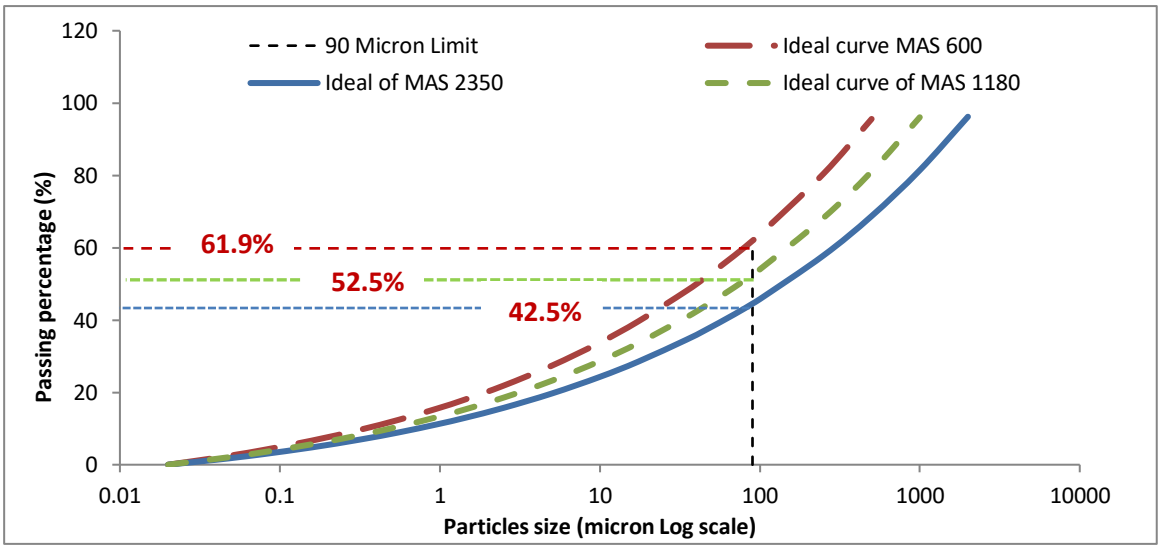

Fig 3. Ideal Particle Size Distribution for Mortars as Per Modified Andreassen.

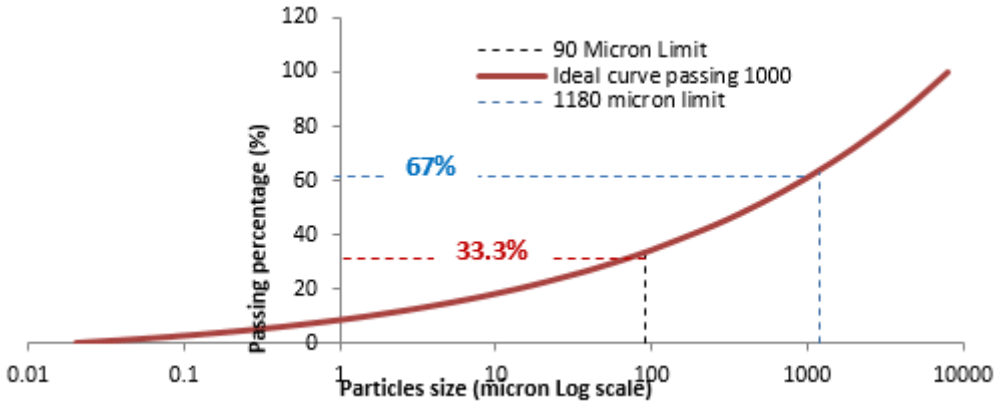

Fig 4. Ideal particle size distribution for HPC as per modified Andreassen

Table 5. Components of HPC by Weight (kg/m^3).

Mix#	C	LS	SF	MK	FA	BA	W	S.P	ST.F	B	W/B
C1	463	153	103	51	702	900	148	15.7	-	770	20%
C2	496	164	110	54	752	750	158	16.8	-	825	20%
C3	529	175	118	58	802	600	169	18.0	-	880	20%
Cs	486	161	108	53	737	735	155	16.5	157	809	20%

C=Cement, LS=Limestone, SF=Silica Fume, MK=Metakaolin, FA=Sand, BA=Basalt aggregate, W=Water, S.P=Superplasticizer, and B= Total binder content.

Table 6. Components of HPC by Volume (%).

Mix#	C(%)	LS(%)	SF(%)	MK(%)	FA(%)	BA(%)	W(%)	S.P(%)	B(%)	B/TP(%)	BA/TP	PV %
C1	14.7	4.8	5.8	2.0	26.5	30	14.8	1.4	27.3	32.6	0.37	43.5
C2	15.8	5.1	6.2	2.2	28.4	25	15.8	1.5	29.3	35.4	0.30	46.6
C3	16.8	5.5	6.6	2.3	30.3	20	16.9	1.6	31.2	38.3	0.25	49.7
Cs*	15.4	5.0	6.1	2.1	27.8	25	15.5	1.5	28.7	35.4	0.30	45.7

C=Cement, LS=Limestone, SF=Silica Fume, MK=Metakaolin, FA=Sand Fine Aggregate, BA= Basalt aggregate, W=Water, S.P=Superplasticizer, B= Total binder content, TP= Total particles volume, and PV= Paste volume.

2.2.2. Phase II: High-Performance Concrete Design

This phase targeted the reduction of the amount of binder material by introducing basalt aggregate as a substitute for mortar. Since the M3 (60M45) mortar mixture produced the most attractive fresh qualities in Phase I (see Results and Discussion section 3.12), basalt aggregate was incorporated as a substitute for M3 mortar volume at varying proportions of 30%, 25%, and 20% to produce three UHPC mixtures designated as C1, C2, and C3, respectively. A fourth mixture, denoted as Cs, was developed by incorporating a 2% volumetric ratio of steel fiber into mixture C2. The concept of substituting mortar had been established upon the

recognition of the modified Andreassen curve. According to Figure 4, the inclusion of course aggregate led to an increase in the maximum aggregate size, resulting in the pursued reduction in binder content and an overall rise in the total aggregate content. The ideal proportion of coarse aggregate to the total particles was determined to be 33%. According to Tables 5 and 6, mixture C2 exhibited the closest percentage of coarse aggregate to the target specified by the modified Andreassen curve.

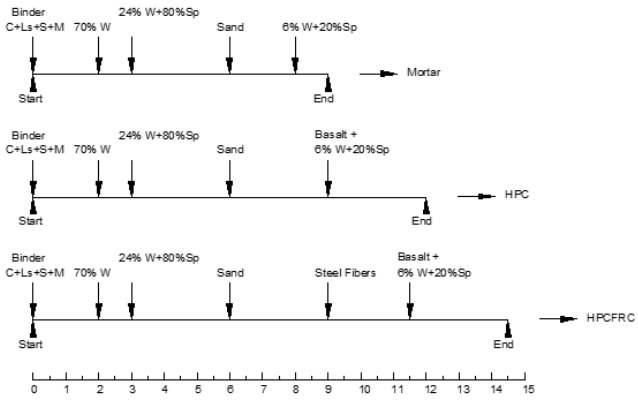

Fig 5. Mixing Regimes for Mixtures.

2.3. *Casting and Curing*

The mixing process was carried out in a pan concrete shear mixer starting with dry mixing of binder components (cement, silica fume, metakaolin and limestone) for 3 minutes to ensure uniform distribution of particles. 70% of the total amount of mixing water was introduced into the mixer, followed by further mixing for 1 minute. 80% of the remaining water, combined with superplasticizer, was added to the mixture with continuous mixing for 3 minutes. Once the paste reached a flowable condition, sand was introduced and mixed for an additional 3 minutes. For mortar mixes, the final remaining mixing water dosage was added at this step. For UHPC mixtures, the last addition of remaining mixing water was postponed until the addition of coarse aggregates, and mixing proceeded for another 3 minutes. The mixing time to produce the UHPC mixture was 12 minutes. Eventually, for the Cs mixture, steel fibers were incorporated before the addition of basalt aggregate and after the insertion of sand, causing an extra 2.5 minutes of mixing time. Figure 5 shows the mixing regimes for various mixtures. Cubic, cylindrical and disc specimens were cast for various mixtures. Concrete was poured into each mold in three successive layers, and each layer was subjected to gentle vibration to eliminate any trapped air pockets. Following the finishing of the concrete surface, specimens were covered with plastic sheets to prevent water evaporation from the specimens, specimens were demolded after 24 h of casting and moved to the respective curing regime. Three curing regimes were applied for specimens reserved for compressive strength namely, standard curing in a water tank (24°C ± 2°C) until the age of testing, hot curing regime (full submersion of specimens in hot water (60°C ± 2°C) for 3 days followed by standard curing until testing) or steam curing regime (in a steam room (90°C ± 2°C) for 3 days followed by standard curing until testing). Curing continued until the age of testing for 7 and 28 days. The rest of the specimens (cylinders and prisms) were cured following the standard curing regime.

2.4. *Testing*

2.4.1. Slump and Slump Flow Testing

Consistency of concrete was determined through slump as per ASTM C143/C143M [26] and slump flow testing (as per BS EN 12350-8) [27], which serve as a measure of ease of concrete mixing, placement, consolidation, and finishing while maintaining suitable uniformity.

2.4.2. Compressive strength

Following the designated curing period, the compressive strength test was performed according to ASTM C109 [28] on three replicate cubic specimens. The size of cubes was 100×100×100 mm for mortar and concrete specimens, respectively. The testing machine had a capacity of 3000 kN capacity.

2.4.3. Splitting tensile strength

An indirect splitting strength test (known as Brazilian tension) was performed on three cylinders (100×200 mm) from each mixture after curing, as per ASTM C496 [29]. Splitting strength was calculated as $2P/(\pi DL)$ where P is the maximum failure load (N), L is the length of the specimen (mm), and D is the diameter of the specimen (mm).

2.4.4. Flexural strength

The examination of flexural strength was conducted on three prism specimens for each mixture, as specified in ASTM C293 [30]. For mortar specimens (Phase I), prism specimens were 40×40×160 mm, compared to 100×100×500 mm for HPC specimens (Phase II). During flexural testing, specimens were subjected to incremental loading until failure following the three-point loading configuration. Flexural strength, also known as modulus of rupture, was calculated as $1.5\,P \times L/d^3$ (MPa) where P is the maximum applied load in N, L is span length (mm) and d is the depth of specimen at the location of fracture (mm).

3. Results and Discussion

This section provides the obtained results of conducted experiments along with a thorough explanation for the achieved behavior.

3.1. *Mixture Development Analysis*

The majority of UHPC designs are based on the principles of particle packing theory, which aims to decrease the porosity of concrete matrices by using smaller particles to fill the gaps between bigger particles. The attainment of the optimum ratio and effectiveness of HPC configuration may be theoretically achieved via applying a suitable particle packing model (Modified Andreassen model).

3.1.1. Analysis of control mixture

Saif *et al.* [24] used a performance-based design method for developing ultra-high-strength self-compacting concrete divided into two phases: Phase I included 12 mortar mixtures tested for fresh and hardened properties to determine the suitable proportions of mortar prior to incorporating coarse particles in Phase II. Phase I was divided into two groups. Group (1) utilized only fine aggregate whereas Group (2) incorporated 26% quartz powder (*QP*) as a filler material replacing sand. Each set contained either 22% SF or 11% SF combined with 11% MK. Steel and polypropylene fibers were used as reinforcing materials at varying densities of 0-160 kg/m^3 and 0-1.8 kg/m^3, respectively. Table 7 represents the mixture proportions for Phase I. All mixtures were analyzed in accordance with a modified Andreasen packing model as per Figure 7.

Figure 3 shows that to obtain optimum density utilizing sand with a maximum aggregate size of 600 microns, particles smaller than 90 microns by 61% of total particles volume are needed to fill the space between sand particles. The total amount of particles smaller than 90 microns in Group (2) was approximately 63% compared to 49% in Group (1). Thus, mixtures of Group (2) had a higher packing density than those of Group (1), which aligned with higher obtained compressive strength (3-4%). Also, Figure 6, which compares the particle distribution curves of mortars M01, M02, M07 and M08 with 600 microns ideal curve of modified Andreassen theory, elucidated that M01 and M02 had a similar trend and M07 and M08 appeared comparable. Adding QP to mixtures M07 and M08 resulted in the least deviation from the optimal curve, with coefficients of variation of 19% and 18%, respectively, compared to 26% and 25% for mixtures M01 and M02, respectively. Furthermore, introducing MK in addition to SF increased mechanical strength by 9-13% due to the rapid pozzolanic reaction of MK with calcium hydroxide, accelerated hydration of OPC, and greater micro-filler effect resulting from its high surface area. Limiting the maximum size to 10 microns, the size at which all employed SF and MK particles pass, it was possible to demonstrate that the addition of MK also reduced the deviation of M02 and M07 curves from the ideal curve.

In Phase II, Saif *et al.* [25] used a ternary replacement strategy employing limestone, silica fume, and metakaolin to produce self-compacting, high-strength concrete. On three categories, nine mixtures were formulated. Group (1) consisted of three mixtures in which SF and MK were substituted for cement in proportions of 20:0, 15:5, and 10:10. Group (2) considered the same mixtures as Group (1), but additionally 20% of cement was substituted by limestone powder. Group (3) was an update to Group (2), in which 34% of sand was substituted with quartz. Table 8 displays the proportions of the mixture noting that 8.1 kg/m^3 of basalt fiber and 540 kg/m^3 of basalt aggregates are combined in all groups.

Utilizing a continuously modified Andreassen curve limited to a maximum aggregate size of 10 mm, the optimum binder content (particles <90 microns) was around 33.3%. All considered mixtures had binder content higher than ideal one, the ratios were 58%, 52%, and 63% for groups in sequence. Adding coarser aggregates to replace the fine aggregate content while maintaining the binder volume is against the philosophy of packing theory. The main target of the authors was achieving the necessary workability to achieve SCC characteristics; Group (2) has the highest flowability with satisfactory mechanical properties compared to Group (3). The best performance in Group (2) was for mixture M5 (cement was replaced by 20% limestone, 15% SF and 5% MK). This mixture was considered the milestone of the current investigation which aims to develop a cost-effective HPC mixture. Eight mixes were developed in two phases earlier.

Table 7. Mortar Mixes Components for Developed UHSFSCC in Phase I (kg/m^3) [24]

Mix#	G#	C	S	MK	F.A	QP	W	S.P	S.P/B	ST. F	PP. F	Slump diameter (mm)	F_{cu} (MPa)	F_{tu} (MPa)	F_b (MPa)
1	G# 01 (Sand)	900	198	0	1050	0	219.6	36.2	3.3%	0	0	795	91.8	7.95	17.4
2			99	99	1050	0		38.4	3.5%	0	0	705	104.0	8.53	19.6
3			198	0	890	0		37.3	3.4%	160	0	715	113.0	10.59	24.8
4			99	99	890	0		39.8	3.6%	160	0	615	123.9	11.48	27.3
5			198	0	1048.2	0		37.3	3.4%	0	1.8	755	102.3	9.96	23.6
6			99	99	1048.2	0		40.6	3.7%	0	1.8	635	115.2	10.56	26.1
7	G# 02 (Sand + Quartz)	900	198	0	780	270	219.6	39	3.6%	0	0	760	95.5	8.29	18.8
8			99	99	780	270		39.5	3.6%	0	0	670	107.1	8.90	21.4
9			198	0	620	270		40.1	3.7%	160	0	680	117.0	11.16	26.7
10			99	99	620	270		40.6	3.7%	160	0	610	127.6	12.16	29.1
11			198	0	778.2	270		41.7	3.80%	0	1.8	640	105.6	10.37	25.1
12			99	99	778.2	270		42.8	3.90%	0	1.8	560	119.1	11.10	28.1

M#=Mix number, G#=Group number, C=Cement, S=Silica Fume, MK=Metakaolin, F.A=Fine Aggregate with MAS 0.6mm, QP=Quartz Powder, W=Water, S.P=Superplasticizer, S.P/B=Superplasticizer Binder Ratio, ST. F= Steel Fiber, PP. F=Polypropylene Fiber, F_{cu} = cubic compressive strength, F_{tu}= tensile strength, and F_{bu} = flexural strength

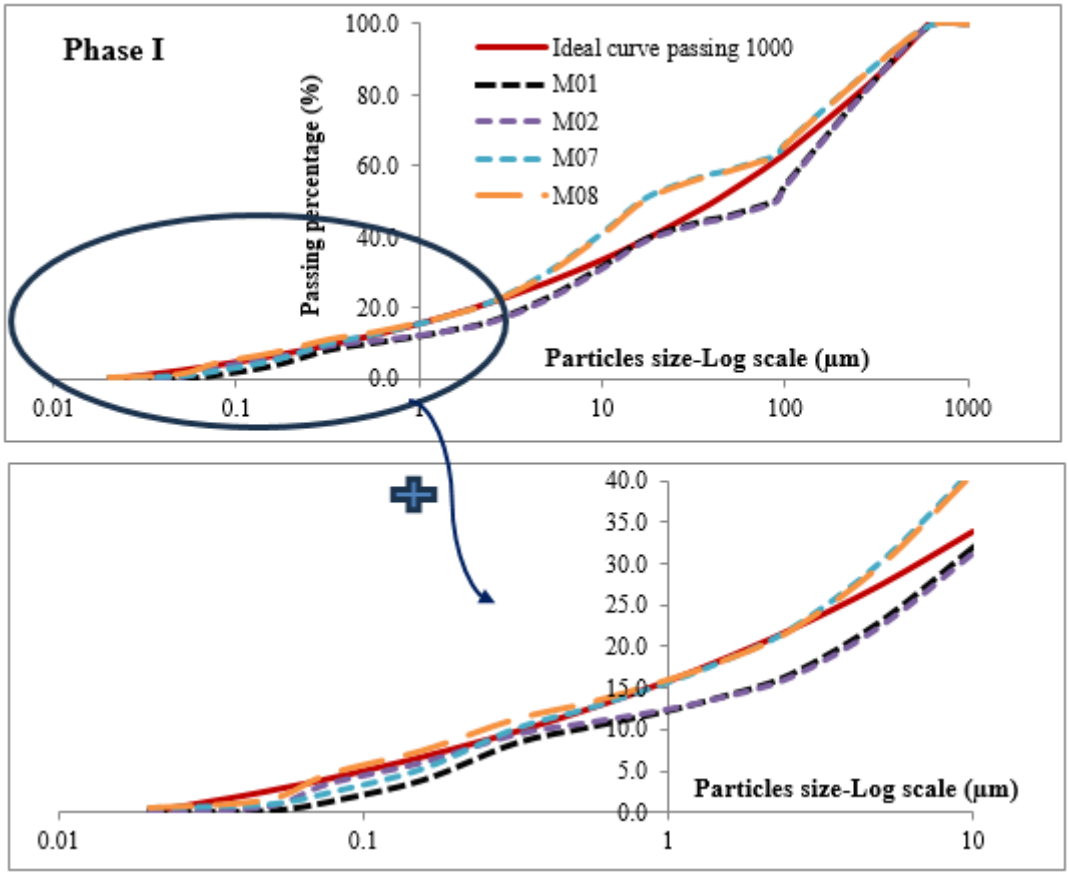

Fig 6. Particle Size Distribution for Mortars in Phase I.

Table 8. Concrete Mixtures (kg/m^3) for Developed UHSBFSCC In Phase II. [25]

M#	Group	C	SF	MK	LS	FA	QP	W	SP	Slump diameter (mm)	F_{cu} (MPa)	F_{tu} (MPa)
M1	G1 QP	880	220	0	0	390	200	200	40	770	120.7	13.6
M2		880	165	55	0	390	200		42	730	124.4	14.6
M3		880	110	110	0	390	200		44	600	115.8	13.1
M4	G2 LS	660	220	0	220	590	0	200	39	800	124.5	14.3
M5		660	165	55	220	590	0		41	780	128.3	15.3
M6		660	110	110	220	590	0		43	730	121.3	14.1
M7	G3 QP+LS	660	220	0	220	390	200	200	41	790	127.1	14.6
M8		660	165	55	220	390	200		43	760	132.3	15.9
M9		660	110	110	220	390	200		45	670	124.2	14.6

M#=Mix number, C=Cement, LS=Limestone, SF=Silica Fume, MK=Metakaolin, FA=Sand Fine Aggregate, QP=Quartz Powder, W=Water, SP=Superplasticizer, G1=group containing QP as sand replacement, G2=group containing LS as inert filler and G3=group containing both QP and LS. F_{cu} = cubic compressive strength, and F_{tu}= tensile strength

Utilizing a continuously modified Andreassen curve limited to a maximum aggregate size of 10 mm, the optimum binder content (particles <90 microns) was around 33.3%. All considered mixtures had binder content higher than ideal one, the ratios were 58%, 52%, and 63% for groups in sequence. Adding coarser aggregates to replace the fine aggregate content while maintaining the binder volume is against the philosophy of packing theory. The main target of the authors was achieving the necessary workability to achieve SCC characteristics; Group (2) has the highest flowability with satisfactory mechanical properties compared to Group (3). The best performance in Group (2) was for mixture M5 (cement was replaced by 20% limestone, 15% SF and 5% MK). This mixture was considered the milestone of the current investigation which aims to develop a cost-effective HPC mixture. Eight mixes were developed in two phases earlier.

3.1.2. Analysis of mortar mixtures design (Phase I)

Four mortar mixtures are designed to optimize the binder content by reducing the cement content and achieving an environmental and economical point of view. Using very fine sand with max. aggregate size (MAS) of 0.6 mm required a high binder content to fill the pores and provide a strong matrix that could hold those particles together, however, limiting the MAS to smaller particles reduced the effect of interfacial transition zones (ITZ) or in other words, micro ITZ was formed which allowed obtaining ultra-high strengths. Figure 7 represents the particles distributions of each mixture versus its target curve and constituents. For optimizing the mix ingredients and getting a clue of appropriate MAS for mortar mixtures, two aggregate sizes were used in Phase I (1118 and 2360 microns) with corresponding total binder content of 42.5% and 52.5% respectively. Subsequently, comparing M2 (50M45) and M3 (60M45) gave a clear vision of the value of obtained characteristics by limiting the MAS versus the cost of each mix. By comparing mixtures M1(50M35) and M2 (50M45), the effect of increasing the SCMs ratios relative to total binder content could be investigated on fresh and hardened properties. The same effect could be checked for mixtures M3 (60M45) and M4 (60M45). The coefficient of variation (COV) was calculated for each mixture using the following equation:

$$RSS = \sum_{i=1}^{n}\left[P_{mix}\left(D_i^{i+1}\right) - P_{Ideal}\left(D_i^{i+1}\right)\right]^2 \quad (2)$$

The results showed that M3 yielded the lowest variation (16%) compared to 17% for both M1 and M2 and 20% for M4

3.1.3. Analysis of HPC mixes design (Phase II)

Following the performance-based approach, the optimum mortar mixture shall serve as the core base of Phase II where the coarse aggregate is introduced. Mixture M03 (60M45) was selected for this phase. The aggregate was added to replace a defined volume from the mortar content as recommended by the continuous particles packing theory philosophy. Figures 8 represent the particles distributions of each mixture versus its target curve and constituents. COV was 17%, 26%, 36% and 26%, respectively for mixture C01, C02, C03 and Cs, respectively.

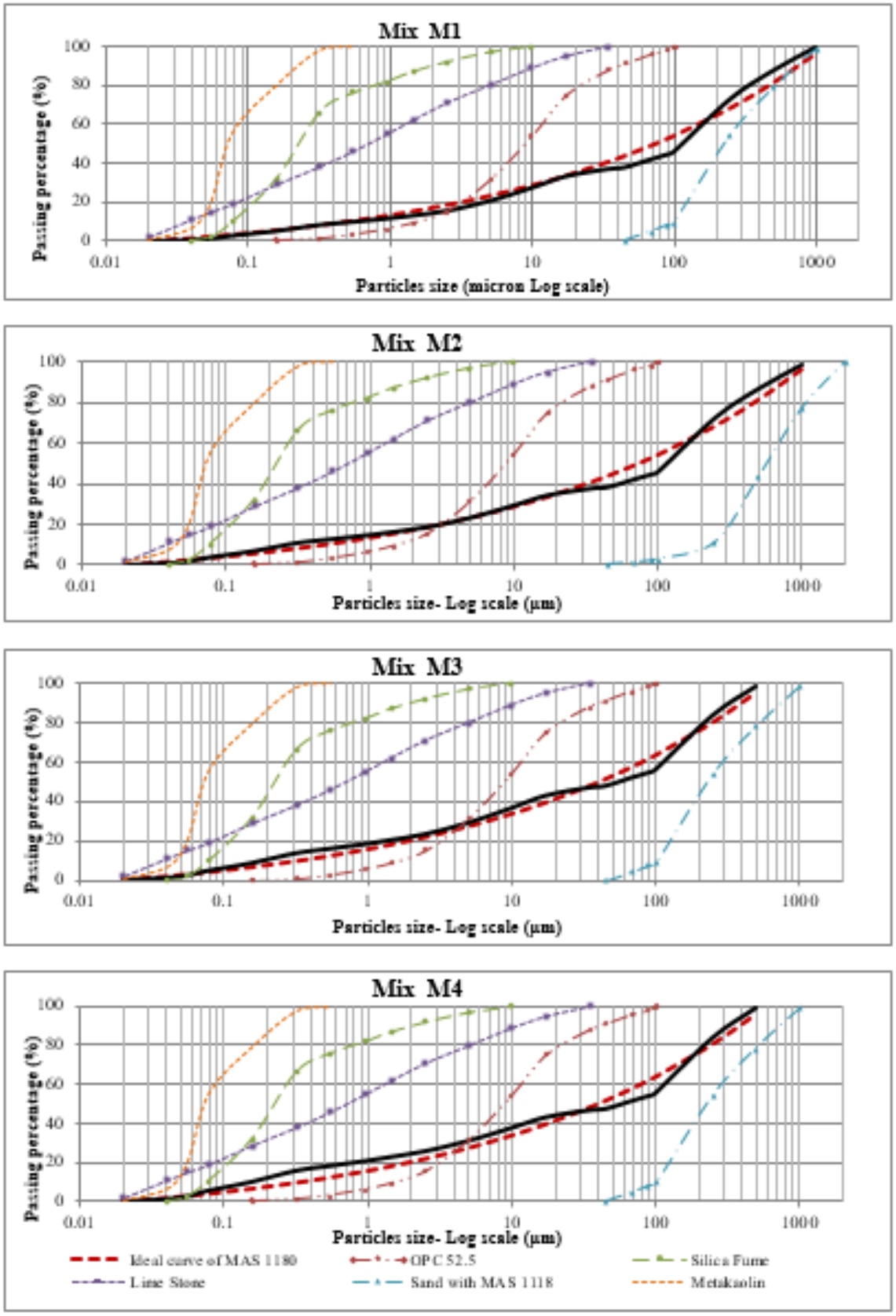

Fig 7. Particle Size Distribution for Mortar Mixes (Phase I).

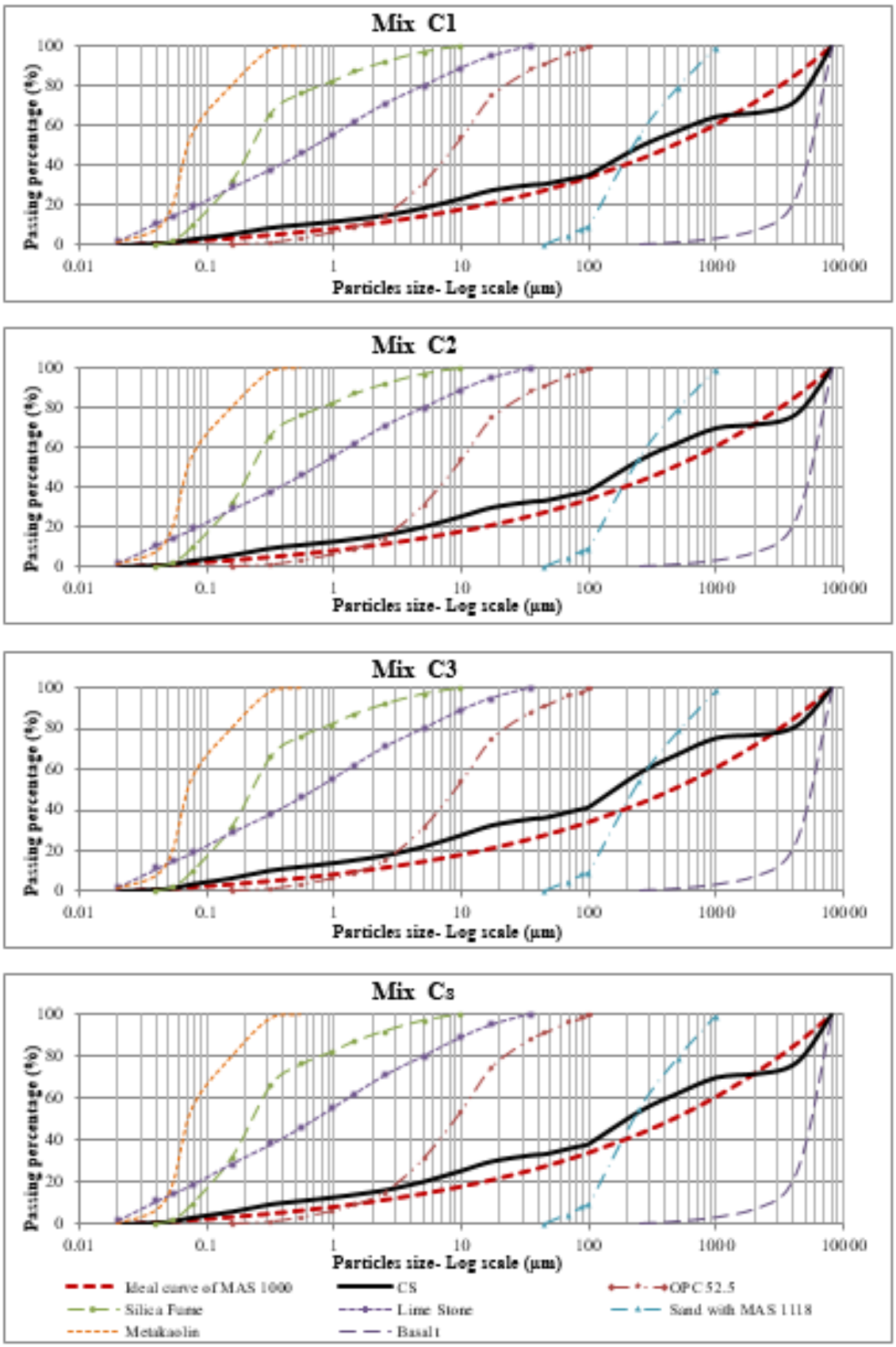

Fig 8. Particle Size Distribution for HPC Mixes (Phase II).

3.2. Fresh Properties

3.2.1. Slump flow test results

The slump flow values for mortar mixtures in Phase I were obtained immediately after mixing with corresponding T50 periods required to attain a slump flow diameter of 50 cm. Figure 9 shows that increasing the binder content had a major role in increasing flowability. Comparing mixtures M2 (50M45) and M3 (60M45) indicated an increase in average slump diameter by 28% while T50 was 13s for mixture 60M45 but failed to be obtained for 50M45. Higher replacement ratios had a negative effect on fresh properties by 8% to 10%. Also, the beneficial effect of limestone powder on fresh properties could not mitigate the decrease in flowability caused by the addition of silica fume and metakaolin. All mixtures met the average slump requirements for self-compacting concretes but T50 values were higher than 10s due to the high viscosity of mixtures. Using modified viscosity agents may solve this issue for further studies.

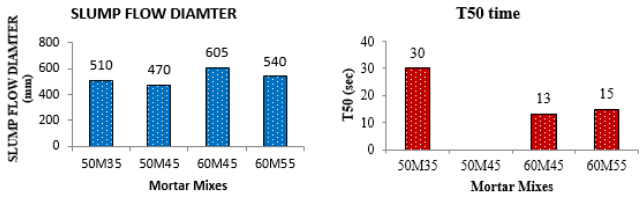

Fig 9. Slump Flow Diameter and T50 Results for Mortar Mixtures.

3.2.2. Standard slump test results

Figure 10 shows the slump of Phase II mixtures. Increasing the coarse aggregate volume decreased slump, yet all mixtures had higher slump values which is acceptable in congested concrete elements. Moreover, the addition of a 2% volumetric ratio of steel fibers result ed in a decrease in the slump by 22% but still in the accepted range for concrete elements.

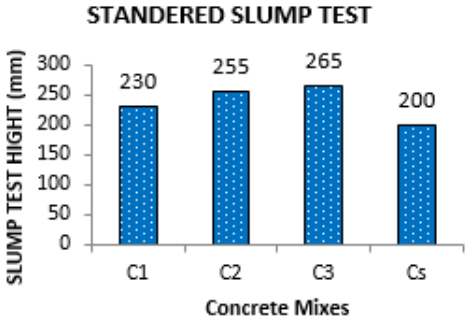

Fig 10. Standard Slump Results for HPC Mixtures.

3.3. *Hardened Properties*

3.3.1. Compressive strength

Standard, hot water and steam curing regimes were adapted after the preparation of compressive strength specimens as per Figure 11. At 7 days, the compressive strength of specimens cured in the standard regime was dependent on cement content such that higher cement content led to a higher early gain of strength. Comparing M1 (50M35) and M2 (50M45), showed that increasing the replacement ratio reduced the cement content by 15% and caused a subsequent decrease in early concrete compressive strength at 7 days by 5%. A similar observation was recorded for M3 (60M45) and M4 (60M55) where the cement content was reduced by 18% and the corresponding early concrete compressive strengths at 7 days decreased by 9%. Continuation of curing until 28 days allowed pozzolanic reactivity to participate in the development of compressive strength such that M1 (50M35) and M2 (50M45) reached comparable strengths. However, the strength of M4 (60M55) was 10% less than that of M3 (60M45) indicating that at high replacement ratios of cement, SCMs may not contribute fully to the strength of the matrix due to the existence of unreacted particles. After 90 days of curing, the strength of M2 (50M45) was 3% higher than that of M1 (50M35) implying the efficiency of replacement up to 45% by volume. Comparatively, the strength of M4 (60M55) was 5% less than that of M3 (60M45), which remarked that continuous curing from 28 to 90 days had a significant impact on enhancing the final gained strengths since the strength gap decreased from 10% at 28 days to 5% at 90 days.

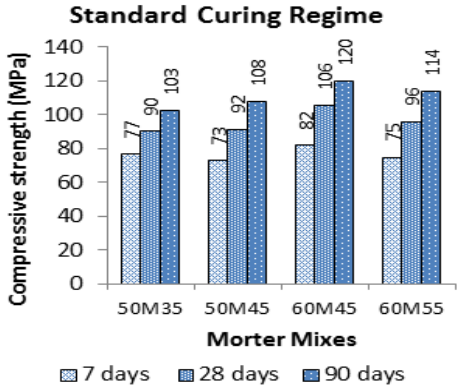

(a)

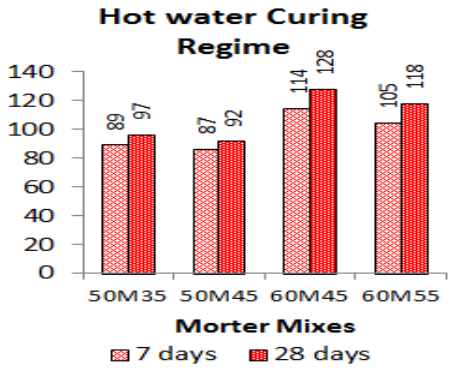

(b)

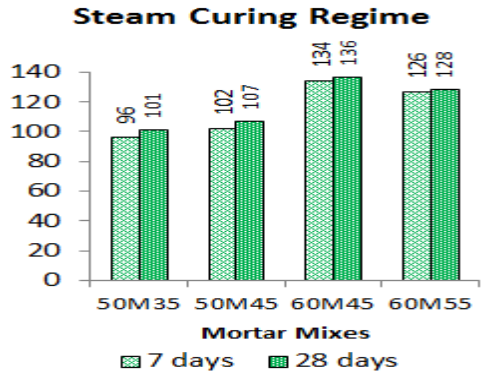

(c)

Fig 11. Compressive Strength for Mortar Mixtures.

Using hot or steam curing regimes accelerated the initial chemical reactions and enhanced the microstructure and compactness of mixtures [31]. As per Figures 11-b and 11-c, strength results obtained at 7 days were nearly equal to or higher than those obtained for specimens cured by the standard method for 28 days. Hot and stream curing regimes allowed mixtures with high replacement ratios M3 (60M45) and M4 (60M55) after 28 days to exceed the achieved strengths at 90 days using the standard curing regime, where the concrete compressive strengths increased by 6% and 3.5% respectively for the hot curing regime and increased by 14% and 13% respectively for steam curing regime. The results obtained after 7 days using steam curing regime were close to the maximum obtained results for all mixtures regardless of the percentage of SCMs.

HPC mixtures in Phase II focused on the effect of basalt aggregate and steel fibers addition. Increasing the aggregate content reduces the cost of the HPC mix and eliminates the hazard effect of shrinkage. Thus, it is necessary to determine the optimum amount of basalt to not compromise fresh and mechanical properties. Figure 10 showed that the slump was reduced by 12% for mixture C2 (contains 25% aggregate) when compared to C3 (contains 20% aggregate), however the strength was nearly the same as shown in Figure 12. On the other hand, both the workability and concrete compressive strength were reduced for mixture C1 (contains 30% aggregate) when compared to C2 by 4% and 6%, respectively. Since the slump was slightly affected and remained within the acceptable levels for all mixtures to cast concrete elements, mixture C2 was the optimum mixture among C1, C2, and C3 where the highest strength was obtained with relatively lower cost and total cement content not exceeding 500 kg/m^3.

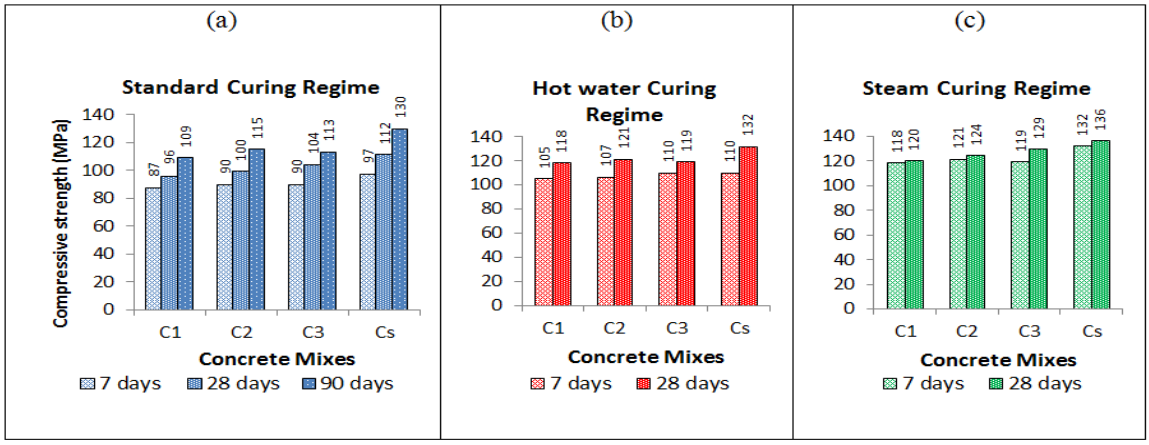

Fig 12. Compressive Strength for HPC Concrete Mixtures

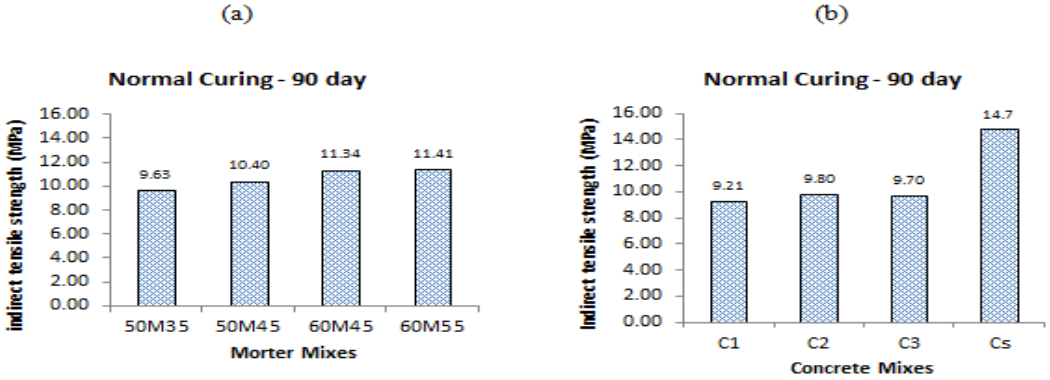

Fig 13. Indirect tensile strength for normal curing at 90 days.

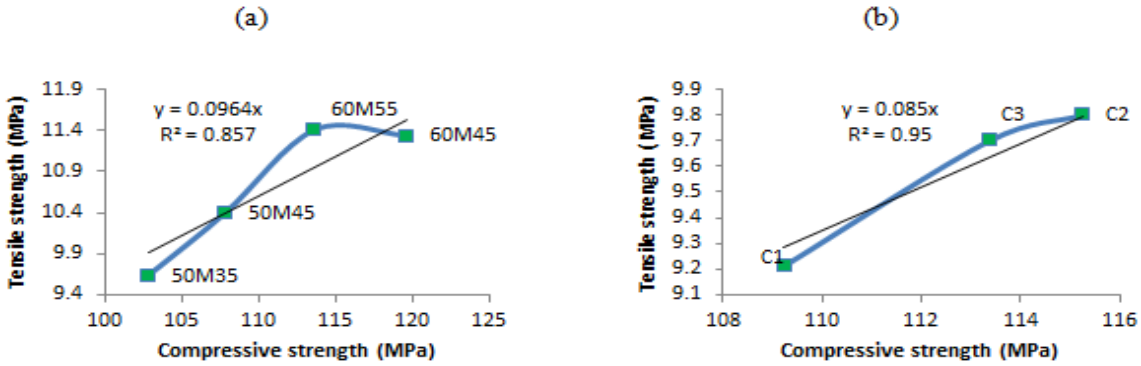

Fig 14. Relation Between Mixes Indirect Tensile Strength and Compressive Strength

Results of tested specimens cured by hot, or steam curing regime provided the same conclusion where the compressive strength of mixture C2 was nearly equal to that of C3. Both hot and steam curing accelerated the rate of compressive strength gain where the results obtained at 28 days were equal or higher than that obtained by the standard curing regime at 90 days (Figures 12-B &12.-C). The addition of steel fibers increased the final concrete compressive strength by 13%, 10%, and 3% for standard, hot, and steam curing regimes, respectively.

3.3.2. Indirect tensile strength

Indirect tensile cylinders (100 mm diameter and 200 mm length) were tested under standard curing at the age of 90 days. Figure 13 shows the indirect tensile strength values for each mix. The indirect tensile strength was proportional to compressive strength as per Figure 14-a, and it also seemed related to the percentage of fines. Increasing the homogeneity of the matrix resulted in higher tensile stress resistance. The ratio between tensile strength and compressive strength was between 9% to 10% depending on the fine percentages. Mixture M4 (60M55) had relatively higher tensile strength than mixture M3 (60M45) although its compressive strength was relatively lower. Incorporating coarse aggregates into mortar M3 (60M45) reduced the tensile strength of mixes C1, C2, and C3 by 14-19%. The addition of steel fibers increased the tensile stresses of mixture C2 by around 50%. Figure 14-b represents the relation between indirect tensile stresses and compressive strength of Phase II mixtures (except Cs), where the addition of aggregate adversely affected the ratio of tensile stresses to 8.5% instead of 9.5% for mortar mixes. The reduced aggregate percentage in mixture C3 (20% by volume) increased the tensile stresses ratio to be above the trend line average.

3.3.3. Flexural strength

The results of mortar prisms tested using a three-point loading flexure test are shown in Figure 15-a. The results aligned with the same behavior remarked for indirect tensile stresses as the flexure strength was not only proportional to compressive strengths, but also increased by improving the mixture homogeneity by increasing the binder percentage. Concrete beams were tested using a three-point loading flexure test for Phase II as shown in Figure 15-b. The flexural strength of mixture M3 (60M45) dropped by 30% to 35% as coarse aggregate was added to the mixture. As shown the addition of steel fibers normalizes the reduction in flexure strength due to the addition of coarse aggregate. As per Figure 16, the ratio of gained flexure strength to compressive strength was about 19% for mortar mixtures and 14% for UHPC mixtures.

3.3.4. Optimization of UHPC ingredients versus its performance.

One of the aims of the current investigation was to develop a cost effective UHPC mixes. Figure 17 reflects the relation between UHPC features and the optimized ingredients in terms of binder content, cement content, and superplasticizer dosage. The reference mixture is the unity, and it shall be noted that this reference mix contains 0.35% of basalt fibers. As per Table 7, a 0.07% of basalt fibers enhanced the compressive strength and tensile strength of mixture M6 when compared to mixture M2 by 10% and 23%, respectively. Except for mix Cs that contained 2% of steel fibers, all mixtures did not include fibers. However, Mixture M3 had a higher concrete compressive strength and mixtures M4, C2 and C3 were comparable. The apparent reduction in compressive strength for mixtures M2 and M1 by 28% and 17% may be enhanced by addition of fibers. The superplasticizer dosage optimized to its 40% of the control mix as the target of the developed mixes was to obtain satisfactory workability for concrete elements and not to produce self-compacted concrete although the current

mixes may reach the self-compacted concrete requirements by appropriate design for admixtures type and dosages without disturbing the particles distribution. The slump diameter was reduced by 20% for design mixture M3 due to the optimization of 50% of superplasticizer dosage. Changing the particle size distribution for mixtures M1, M2 and M4 resulted in a small variance in slump diameter. However, Mixture M3 was selected based on its high performance, attention shall be made for mix M4, it obtained almost the same target compressive strength of control mixture with optimized cement content 16% lower than the control mixture. The addition of basalt aggregates optimized the powders and cement contents by the same substitution ratio of basalt aggregates 20, 25, and 30% for mixes C1, C2, and C3, respectively. Comparing the final mixture Cs with control mix, the compressive strength of mixture Cs was higher by 6% and the tensile strength was slightly lower by 4% while the binder content and the cement content were optimized by 26%.

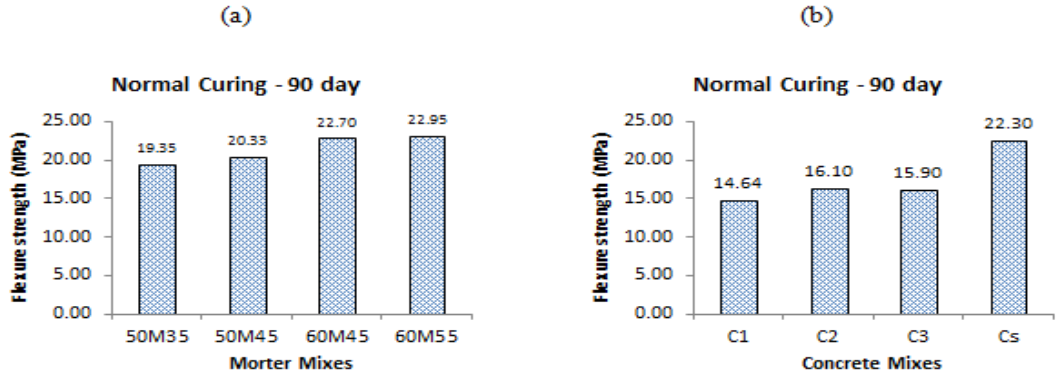

Fig 15. Mortar Flexural Strength for Normal Curing At 90 Days.

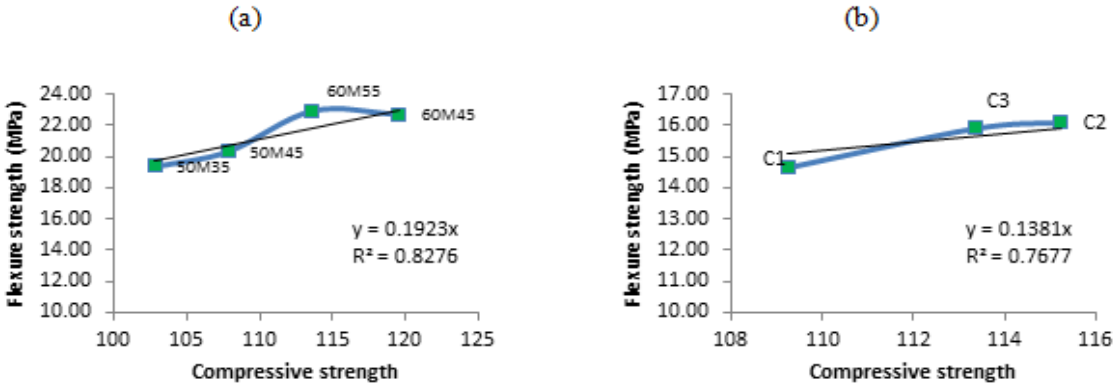

Fig 16. Relation Between Mixes Flexural Strength and Compressive Strength.

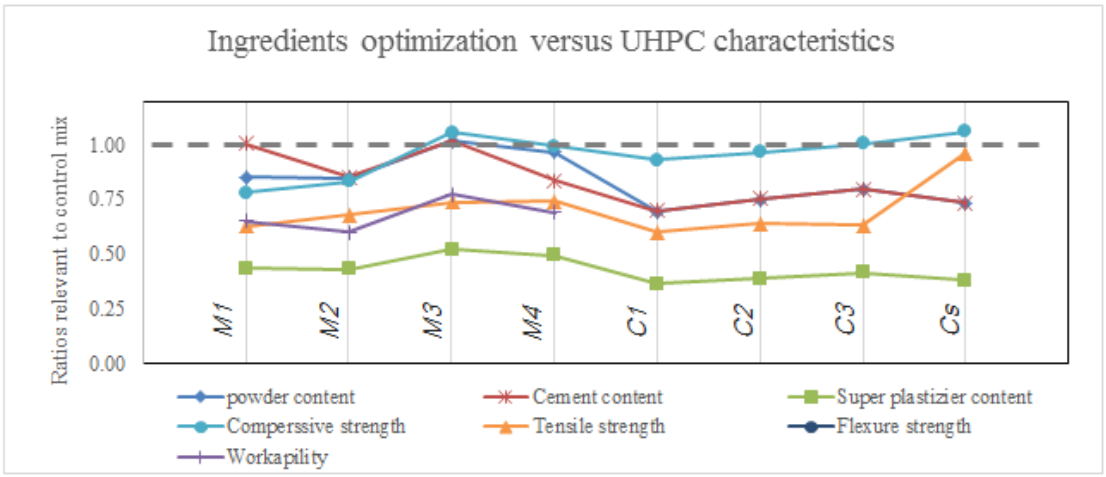

Fig 17. Ingredients Optimization Versus HPC Characteristics

4. Conclusions

The current study investigated a mixed design procedure to develop ultra-high-performance concrete where the modified Andreassen model was used as the framework to quantify the binder, fine aggregate and coarse aggregate contents. A two-step performance-based design was used to select the best performance output of mortar (Phase I) and concrete (Phase II). Based on testing and analysis, the following conclusions can be drawn: -

1- The modified Andreassen model was an effective approach to determine the optimum particle distribution, on which the binder, fine aggregate, and coarse aggregate contents could be evaluated. It was better to select the grading curves of aggregate to achieve the least deviation from the ideal model curves.

2- The ternary replacement of limestone, silica fume, and metakaolin by mass ratio of 3:2:1 produced a dense binding matrix that led to better concrete compressive strength results.

3- At a fixed superplasticizer dosage, increasing the binder content resulted in higher mixture flowability. However, excessive replacement ratios had a negative effect on fresh properties. The beneficial effect of limestone powder on fresh properties could not mitigate the decrease in flowability caused by the addition of silica fume and metakaolin.

4- The early gain in concrete strength was related to the high cement content. However, hot curing regimes were more efficient to accelerate the gain of strength. Results of the steam curing regime at 7 days were comparable to or higher than those of the 90 day normal curing regime.

5- The addition of basalt coarse aggregates optimized the environmental effects and cost impacts since it reduced the binder content by the same volume ratio of the used coarse aggregates. Nonetheless, basalt did not compromise the compressive strength of UHPC.

6- The addition of a 2% volumetric ratio of steel fibers increased the compressive strength of UHPC by 13% while increasing the tensile strength by around 50%.

References

[1] K. Wille, A. Naaman and G. Parra-Montesinos, "Ultra-High Performance Concrete with Compressive Strength Exceeding 150MPA (22KSi): A Simpler Way," *ACI Materials Journal*, vol. 108, no. 1, pp. 46-54, 2011.

[2] D.-Y. Yoo and N. Banthia, "Mechanical properties of ultra-high-performance fiber-reinforced concrete: A review," *Cement and Concrete Composites*, vol. 73, pp. 267-280, 2016.

[3] P. A€ıtcin, "The durability characteristics of high performance concrete: a review," *Cement and Concrete Composites*, vol. 25, pp. 409-420, 2003.

[4] O. T. Sanya and J. Shi, "Ultra-high-performance fiber reinforced concrete review: constituents, properties, and applications," *Innovative Infrastructure Solutions*, vol. 8, no. 188, 2023.

[5] ACI-239R-18, "Ultra-High-Performance Concrete: An Emerging Technology Report," American Concrete Institute, USA, 2018.

[6] Y. Li and J. Li, "Capillary tension theory for prediction of early autogenous shrinkage of self-consolidating concrete," *Construction and Building Materials*, vol. 53, no. 28, 2014.

[7] T. Buttignol, J. Sousa and T. Bittencourt, "The Path to Ultra High Performance Fiber Reinforced Concrete (UHPFRC): Five Decades of Progress.," in *Brazilian Conference on Composite Materials*, Brazil, 2018.

[8] D. Fan, J. Zhu, M. Fan, S. C. Jian-Xin Lu, E. Dong and R. Yu, "Intelligent design and manufacturing of ultra-high performance concrete (UHPC) – A review," *Construction and Building Materials*, vol. 385, no. 131495, 2023.

[9] A. Tafraoui, G. Escadeillas, S. Lebaili and T. Vidal, "Metakaolin in the formulation of UHPC," *Construction and Building Materials*, vol. 23, pp. 669-674, 2009.

[10] N. A. Soliman and A. Tagnit-Hamou, "Using Particle Packing and Statistical Approach to Optimize Eco-Efficient Ultra-High-Performance Concrete," *ACI Materials Journal*, vol. 114, no. 6, 2017.

[11] W. Huang, H. Kazemi-Kamyab, W. Sun and K. Scrivener, "Effect of replacement of silica fume with calcined clay on the hydration and microstructural development of eco-UHPFRC," *Materials & Design*, vol. 121, no. PP 36-46, 2017.

[12] L. Chenzhi, "Mechanical and transport properties of recycled aggregate concrete modified with limestone powder.," *Composites Part B: Engineering*, vol. 197, no. 108189, 2020.

[13] E. Berodier, K. Scrivener and G. Scherer, "Understanding the Filler Effect on the Nucleation and Growth of C-S-H," *Journal of the American Ceramic Society*, vol. 97, no. 12, 2014.

[14] J. Ma, M. Orgass, F. Dehn, D. Schmidt and N. Tue, "Comparative Investigations on Ultra-High Performance Concrete with or without Coarse Aggregates," in *Proc. Int. Symp. Ultra High Perform. Concr.*, Kassel., 2004.

[15] P. Li, Q. Yu and H. Brouwers, "Effect of coarse basalt aggregates on the properties of Ultra-high Performance Concrete (UHPC)," *Construction and Building Materials*, vol. 170, p. 649–659, 2018.

[16] R. Kozul and D. Darwin, "Effects of Aggregate Type, Size, and Content on Concrete Strength and Fracture Energy," in *The national science foundation*, Lawrence, Kansas, 1997.

[17] R. Yu, P. Spiesz and H. Brouwers, "Mix design and properties assessment of Ultra-High Performance Fibre Reinforced Concrete (UHPFRC)," *Cement and Concrete Research*, vol. 56, pp. 29-39, 2014.

[18] S. J. and G. Xu, "Classification of Ultra-high Performance Concrete UHPC," *European Journal of Engineering and Technology Research*, vol. 6, no. 6, pp. 87-96, 2021.

[19] W. Meng, M. Valipour and K. H. Khayat, "Optimization and Performance of Cost-Effective UltraHigh Performance Concrete.," *Materials and Structures*, vol. 50, no. 29, 2017 (b).

[20] J. Du, W. Meng, K. H. Khayat, Y. Bao, P. Guo and Z. Lyu, "New development of ultra-high-performance concrete (UHPC)," *Composites Part B Engineering*, vol. 224, no. 109220, 2021.

[21] S. Kumar and M. Santhanam, "Particle packing theories and their application in concrete mixture proportioning: A review," *The Indian Concrete Journal*, vol. 77, no. 9, pp. 1324-1331, 2003.

[22] M. Safiuddin, H. Al-Mattarneh and M. Zain, "Analytical study on the

slump of fresh high performance concrete using finite element method.," *Journal of International Association for Concrete Technology.*, vol. 8, pp. 81-90, 2003.

[23] R. O'Hegarty, O. Kinnane, J. Newell and R. West, "High performance, low carbon concrete for building cladding applications," *Journal of Building Engineering*, vol. 43, no. 102566, 2021.

[24] M. S. Saif, A. S. Shanour, G. E. Abdelaziz and M. S. Hammad, "Characteristics of Ultra-High-Strength Self-Compacting Concrete (UHSSCC) Containing Macro Steel, Polypropylene Fibers and Local Materials," *Engineering Research Journal - Faculty of Engineering (Shoubra)*, vol. 52, no. 1, pp. 18-26, 2023.

[25] M. S. Saif, A. S. Shanour, G. E. Abdelaziz, H. I. Elsayad, I. G. Shaaban, B. A. Tayeh and Mahmoud S. Hammad, "Influence of blended powders on properties of Ultra-High Strength Fibre Reinforced Self Compacting Concrete subjected to elevated temperatures," *Case Studies in Construction Materials*, vol. 18, no. 01793, 2023.

[26] ASTM-C143/C143M, "Standard Test Method for Slump of Hydraulic-Cement Concrete," ASTM International, America, 2020.

[27] BS-EN:12350-8, "Testing fresh concrete. Self-compacting concrete - slump-flow test," British Standards Institution, London, 2019.

[28] ASTM-C109, "Standard Test Method for Compressive Strength of Cube Concrete Specimens," American Society for Testing and Materials Standard Practice C109, Philadelphia, Pennsylvania, 2004.

[29] ASTM-C496, "Standard Test Method for Splitting Tensile Strength of Cylindrical Concrete Specimens," American Society for Testing and Materials Standard Practice C496, Philadelphia, Pennsylvania, 2017.

[30] ASTM-C293, "Standard Test Method for Flexural Strength of Concrete (Using Simple Beam with center-Point Loading)," American Society for Testing and Materials Standard Practice C293, Philadelphia, Pennsylvania, 1994.

[31] N. N. Melekaa, A. A. Bashandy and M. A. Arab, "Ultra High Strength Concrete Using Economical Materials," *International journal of current engineering and technology*, vol. 3, no. 2, 2013.